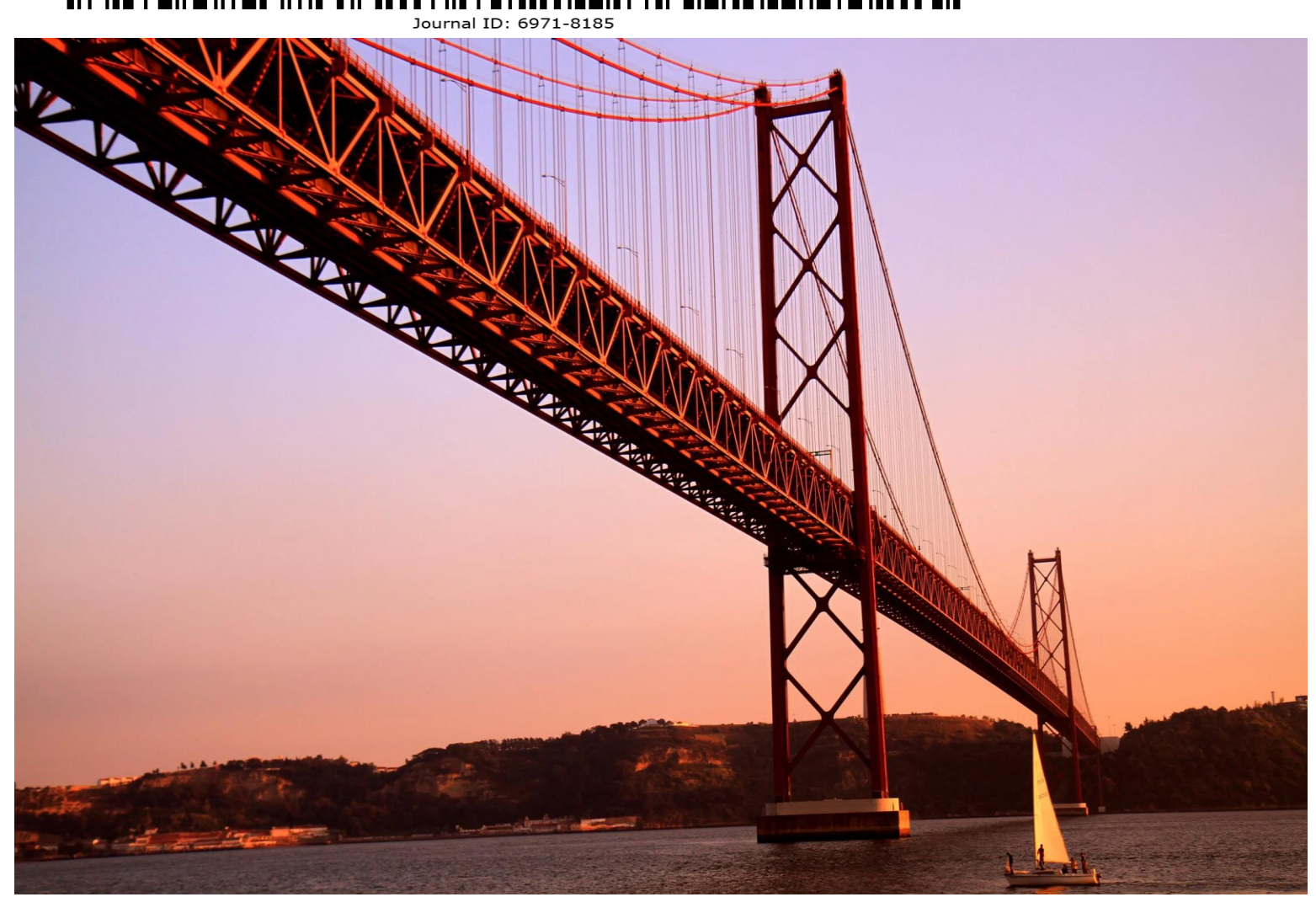






INTERNATIONAL JOURNAL OF CIVIL ENGINEERING AND TECHNOLOGY





IAEME Publication

Chennai, India editor@iaeme.com/ iaemedu@gmail.com



International Journal of Civil Engineering and Technology (IJCIET)

Volume 16, Issue 5, September-October 2025, pp. 35-55, Article ID: IJCIET_16_05_003 Available online at https://iaeme.com/Home/issue/IJCIET?Volume=16&Issue=5

ISSN Print: 0976-6308 and ISSN Online: 0976-6316

Impact Factor (2025): 21.69 (Based on Google Scholar citation)

Journal ID: 6971-8185; DOI: https://doi.org/10.34218/IJCIET 16 05 003



EXPERIMENTAL INVESTIGATION OF LEAKAGE-PRESSURE RELATIONSHIPS IN WATER DISTRIBUTION SYSTEMS: EFFECTS

Majed O. Alsaydalani¹

OF SURROUNDING MEDIA AND ORIFICE SIZE

¹Civil Engineering Department, College of Engineering and Architecture, Makkah, Saudi Arabia.

ABSTRACT

Leakage in water distribution systems (WDS) continues to impose substantial economic and environmental costs worldwide. Although leakage is often modeled using the orifice equation with a square-root dependence on pressure, these representations typically assume free discharge conditions and rarely account explicitly for the surrounding medium. This paper presents a controlled laboratory study that quantifies how surrounding media—air, water, and saturated sand—modulate leakage rate, discharge coefficient, and the leakage—pressure relationship for small circular openings. Four steel pipe test sections (12 mm internal diameter) with orifices of 1, 3, 6, and 9 mm were evaluated over pressures up to 70 kPa. The apparatus ensured single-orifice flow, accurate pressure measurements via a calibrated gauge, and repeatable data collection. Results show that discharging into water produces leakage trends comparable to free discharge into air, with leakage approximately proportional to pressure to the 0.5 power and discharge coefficients $C_d \approx 0.6$ –0.7. In contrast, discharging into saturated sand dramatically attenuates leakage—frequently by an

OPEN ACCESS

order of magnitude relative to air—and reduces the effective discharge coefficient by up to $\sim 93\%$ (e.g., C_d falling from ~ 0.65 to ~ 0.045 for a 3 mm orifice). Moreover, the soil case exhibits a near-linear pressure—leakage relation up to a threshold ($\sim 30-40$ kPa), beyond which disproportionate increases in flow are observed and soil piping initiates (noted near ~ 32 kPa for a 9 mm orifice). These findings challenge the notion that surrounding soil has negligible impact on leakage and underscore the need to incorporate media effects into leakage modeling, pressure management, and risk assessment.

Keywords: leakage, pressure management, discharge coefficient, orifice flow, soil piping, water distribution systems, sandy soils, experimental hydraulics

Cite this Article: Majed O. Alsaydalani. (2025). Experimental Investigation of Leakage–Pressure Relationships in Water Distribution Systems: Effects of Surrounding Media and Orifice Size. *International Journal of Civil Engineering and Technology* (*IJCIET*), 16(5), 35-55. DOI: https://doi.org/10.34218/IJCIET_16_05_003

1. Introduction

Non-revenue water (NRW) due to leakage remains a central challenge for utilities, affecting financial sustainability, service reliability, and environmental stewardship. Conventional pressure—leakage formulations—rooted in the orifice equation—implicitly assume free discharge conditions and treat the surrounding medium as inconsequential. In buried pipes, however, water escapes into a soil matrix whose permeability, gradation, compaction state, and stress history can substantially modify leak hydraulics and failure modes.

Prior studies in urban water systems often report pressure—leakage exponents near 0.5 for rigid, circular orifices, but exponents N > 1 are also documented when deformable leak paths, joints, or cracks expand with pressure. Less well quantified is how the environment into which the leak discharges (air, water, or saturated soils) reshape the leakage—pressure curve and alters the discharge coefficient. From a risk perspective, upward seepage in sand can mobilize grains and trigger internal erosion and piping, ultimately undermining the ground or leading to sudden increases in leakage.

This research contributes a focused experimental analysis that isolates media effects (air, water, saturated sand) and orifice size (1–9 mm) on leakage behavior under controlled pressure. We quantify (i) absolute leakage rates, (ii) normalized leakage (leakage factor) versus

pressure, (iii) discharge coefficients C_d , and (iv) the onset of soil piping. The results offer evidence-based guidance for leakage modeling and pressure management strategies in sandy ground conditions, directly relevant to network operations and asset risk management.

2. Literature Review

Leakage from water distribution systems (WDS) is both a technical and management problem with direct financial, environmental, and service-reliability implications. Utilities have long recognized that system pressure is a primary driver of real losses, which explains the centrality of pressure management in handbooks and practice guides [1,5,6,19]. In engineering analyses and many network simulators, leakage is frequently modeled using an orifice-based representation in which discharge is proportional to the square root of pressure head, i.e., $Q \propto P^{0.5}$. This treatment originates from classical hydraulics and has been operationalized in network models as a pressure-dependent emitter or leak node [1,10–12]. Yet the generality of the 0.5 exponent is limited, particularly for defects that deform with pressure or when the discharge environment departs from free/submerged conditions.

The Fixed and Variable Area Discharge (FAVAD) concept formalized the idea that leak areas (e.g., cracks, joint gaps) can expand with pressure, producing pressure—leakage exponents N that exceed 0.5, sometimes approaching or surpassing unity [2–4]. From a utility perspective, this means that a modest reduction in average zone pressure can yield disproportionate leakage reduction when N > 0.5. The practical literature (AWWA M36 and IWA guides) therefore emphasizes both pressure control and field calibration of local leakage—pressure relations [5,6,19].

Laboratory and field studies have provided varied exponents depending on leak type, material, and boundary conditions. For rigid, circular orifices, studies repeatedly recover the classical orifice equation with N \approx 0.5 and discharge coefficients C_d in the neighborhood of 0.6–0.7 under free or submerged conditions, provided that Reynolds numbers are sufficiently high and edges are sharp [11,12]. However, when leaks resemble cracks or slits in deformable materials, the effective opening can widen with pressure, and measured exponents rise: experimental and computational investigations by Greyvenstein & van Zyl, van Zyl & Clayton, and Cassa & van Zyl show that N depends on material elasticity, crack geometry, and confinement, with typical values in the 0.5–1.5 range [7–9]. These findings underpin modern formulations in which the head–leakage slope and the apparent exponent are treated as parameters to be calibrated, rather than constants to be assumed.

Computational tools used for calibration (e.g., EPANET-based models) allow leakage emitters to be linked to pressure zones, facilitating multi-scenario testing of pressure set-points, diurnal demand, and valve configurations [10]. Still, translating small-scale laboratory coefficients into district-scale emitter parameters remains nontrivial: internal pipe approach conditions, local turbulence, and boundary layers can alter the vena contracta, while external environments (submergence, soil confinement) can add losses not captured by purely free-jet assumptions.

A major simplification in many leakage models is the implicit assumption of discharge into air (free jet). For submerged discharge into water, textbooks report that C_d for small, sharpedged circular orifices remains broadly similar to free conditions (typically 0.6–0.7), especially at higher heads where entrance losses dominate [11,12]. This has encouraged the practice of applying orifice-based relations even when the exterior is water-filled, with calibration absorbing small differences.

However, buried networks typically discharge into saturated soil, not open water. In such cases, the escaping jet must traverse a porous skeleton and pore water, which can (i) disrupt jet coherence, (ii) reduce the effective opening area (by particle intrusion or local arching at the orifice), and (iii) impose additional head losses through seepage paths. The outcome is an apparent reduction in C_d and a steeper pre-threshold pressure–leakage slope than predicted by the square-root law. When hydraulic gradients become large enough, upward seepage can mobilize particles and induce internal erosion and piping, producing sudden, disproportionate increases in leakage with concurrent pressure collapse—phenomena reported in soil mechanics and dam engineering [13–17].

Mechanistically, the key contrast with free and submerged discharge is that the soil skeleton stores and dissipates energy. Prior to critical hydraulic gradient, the soil adds resistance, suppressing leakage and effectively linearizing the pressure–leakage curve. At and above the piping threshold, the structure progressively destabilizes; "boiling" and channel formation reduce resistance rapidly, flipping the system into a high-leakage state. Classical soil mechanics teaches that the critical gradient i_c scales with submerged unit weight and gradation; angular, well-graded sands often exhibit higher resistance to mobilization than rounded, uniformly graded sands due to interlocking [15,16].

Besides the external medium, orifice geometry and the orifice-to-pipe diameter ratio influence observed coefficients. Even in air, larger orifices can display slightly lower C_d due to differences in contraction and approach flow conditions within the carrier pipe [11,12]. The

internal Reynolds number (based on mean exit velocity and orifice diameter) typically falls in the turbulent regime for practical leak heads, but transition and scaling effects are not negligible for 1–2 mm micro-orifices at low heads. In buried settings, larger openings deliver higher momentum flux into the soil, enhancing grain rearrangement and increasing the likelihood of crossing the piping threshold at a given pressure. Conversely, very small openings (e.g., 1 mm) behave as strong hydraulic resistors; most head loss occurs across the orifice, so external medium effects are muted. These qualitative trends align with experimental reports demonstrating stronger medium sensitivity for larger orifices and comparatively minor differences for the smallest orifices in the same apparatus.

At network scale, pressure management strategies—PRVs, district metering, and time-of-day set-points—aim to "flatten" pressures while keeping service levels acceptable. The practitioner's literature (AWWA M36; Farley & Trow; Thornton et al.) translates physics into actionable controls: (i) reduce average and peak pressures to lower real losses, (ii) prioritize zones with high night flows and sandy backfills, and (iii) monitor for threshold behavior (abrupt flow rises at nearly constant pressures) suggestive of internal erosion [5,6,19]. Recent reviews synthesize diagnostic methods—acoustics, transients, night-flow analysis—and highlight the need for site-specific calibration of exponents and coefficients due to variability in pipe materials, defect types, and soil conditions [18].

Despite extensive work on leak hydraulics and pressure management, there remain two persistent gaps relevant to buried pipes:

- Controlled comparisons of free, submerged, and saturated-soil discharges for the same orifices, materials, and pressures are scarce. Studies often focus on free/submerged cases or on deforming cracks in isolation, leaving the soil-discharge case underquantified.
- 2. The pre- and post-threshold behavior in sand—manifesting as (a) suppressed, quasilinear leakage growth at subcritical gradients and (b) disproportionate increases upon piping—is insufficiently embedded in routine leakage models used by utilities.

The present study addresses these gaps with side-by-side experiments using 1–9 mm circular orifices, a consistent internal approach flow (12 mm steel pipe), and three external media (air, water, saturated sand). The results (i) verify the similarity of free and submerged discharge, (ii) quantify the order-of-magnitude reduction in apparent C_d in saturated sand, (iii) demonstrate medium-dependent exponents (\approx 0.5 in air/water vs \approx 1 pre-threshold in sand), and (iv) document the onset of piping and its hydraulic signature. Together, these insights inform

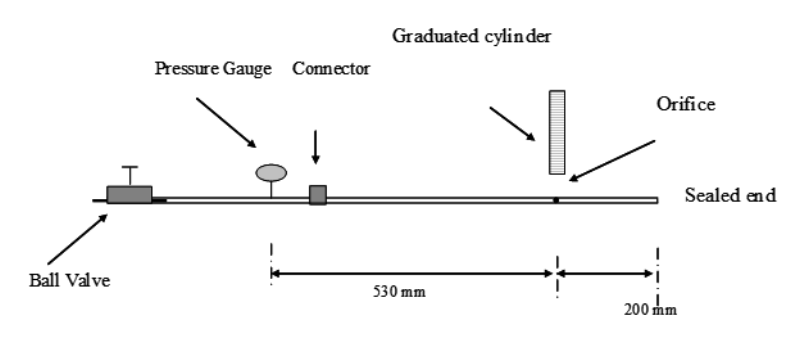
improved parameterization of leakage in buried conditions and support risk-aware pressure management where sandy soils prevail.

3. Materials and Methods

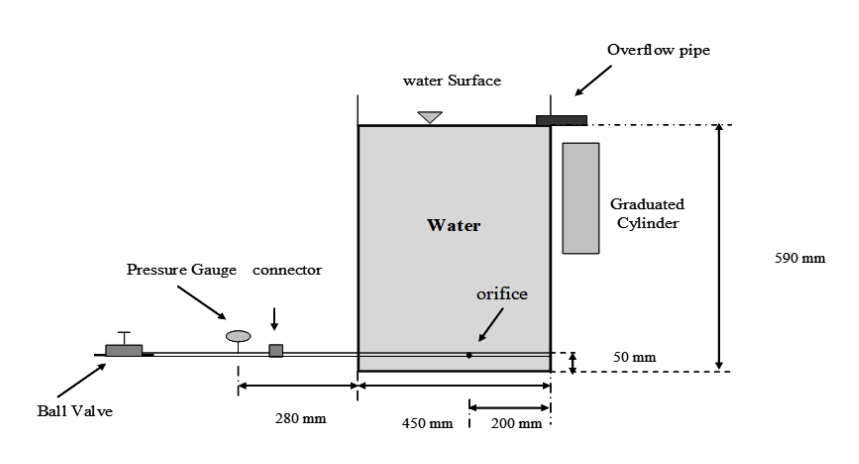
3.1. Experimental set-up

A prototype laboratory model was designed and constructed to investigate the influence of the surrounding medium and orifice characteristics on leakage from pressurized pipes. The apparatus comprised a cylindrical container (height: 65 cm; inner diameter: 45 cm) and four test sections fabricated from 12 mm-diameter steel pipe with a uniform wall thickness of 3 mm. Each test section contained a single circular orifice with diameters ranging from 1 mm to 9 mm.

One end of each test section was connected to a pressurized supply hose fed from a constant-head reservoir (water butt with maintained water level); the downstream end was sealed with a cap, such that discharge occurred only through the orifice. A lever-type ball valve regulated inflow and system pressure. A pressure gauge, mounted immediately upstream of the test section, provided local pressure readings; due to apparatus limitations, the maximum measurable pressure was 70 kPa. An overflow line installed near the top of the container routed excess water to a graduated cylinder for volumetric measurement (Figure 1).



(a) discharge into air



(b) discharge into water

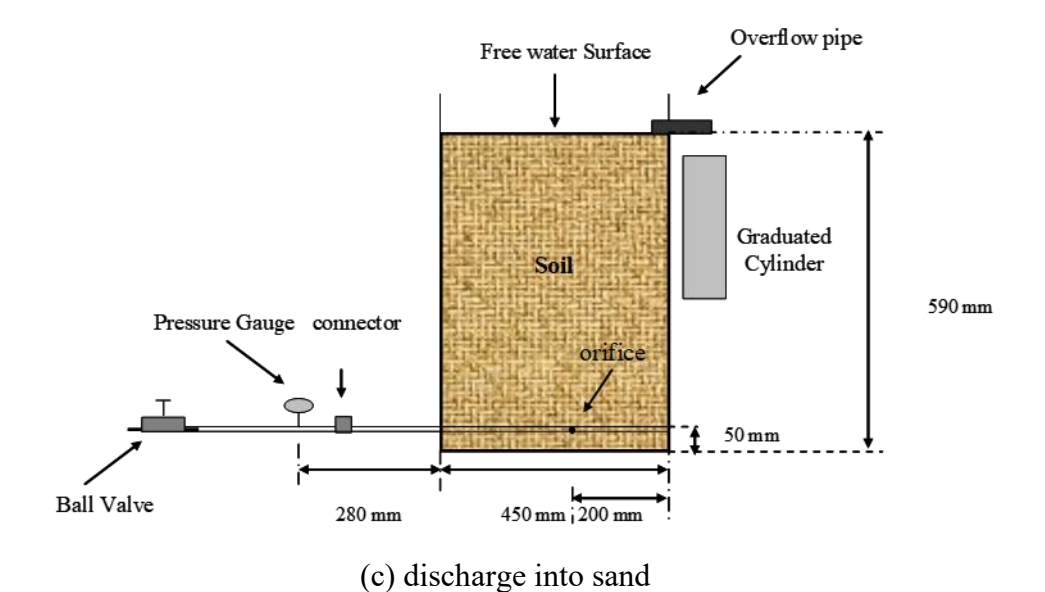


Figure 1 Schematic of the experimental apparatus (a) discharge into air, (b) discharge into water and (c) discharge into sand

Test Media

Experiments were performed under three surrounding media: air, water, and saturated sand. The soil used in the saturated-medium tests was a well-graded sand (particle size range: 0.06–5.0 mm) with median particle diameter D50 = 0.6 mm and coefficient of uniformity Cu=5.33 Cu=5.33 Cu=5.33. Scanning electron micrographs indicated predominantly angular, irregular particle shapes (Figures 2–3).

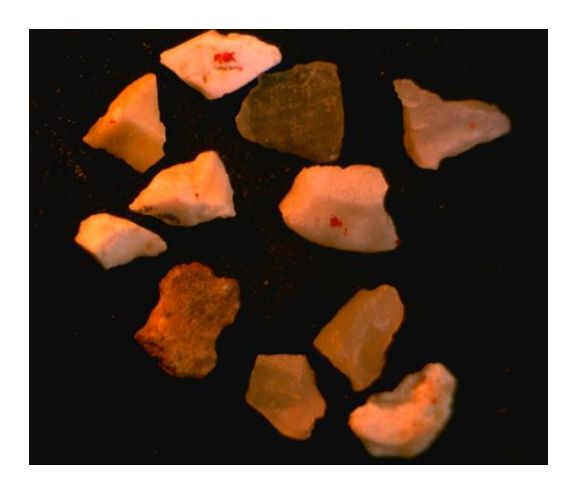


Figure 2 Scanning electron micrograph of the sand

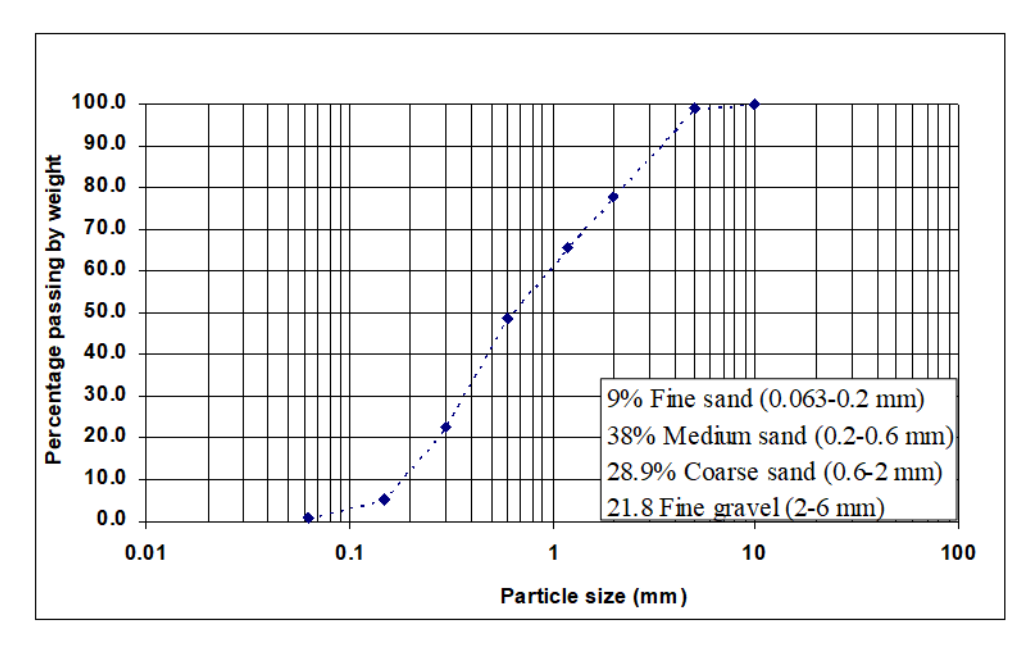


Figure 3 Particle size distribution of the sand (D50 = 0.6 mm; Cu = 5.33); well graded material.

Experimental Procedures

For each pipe section (i.e., each orifice diameter), three tests were conducted—one per surrounding medium—following standardized preparation and measurement protocols:

Discharge into air

The test section was connected directly to the pressurized hose and positioned horizontally (Figure 1a). Prior to data collection, the valve was opened to flush the line until all trapped air was purged and a stable jet formed at the orifice.

Discharge into water

The connected test section was placed horizontally inside the container, which was then completely filled so that the pipe was submerged beneath a 54 cm water depth (Figure 1b).

Discharge into saturated sand

The test section was positioned horizontally in the container (Figure 1c). The container was first half-filled with water, after which sand was added in layers while gently stirring to minimize air entrapment. The container was subsequently shaken to promote densification and release of residual air, achieving a saturated condition prior to testing.

Data acquisition

In all cases, testing commenced at low pressure and flow, followed by incremental increases in pressure using the ball valve. At each set point, the system was allowed to reach steady conditions before measurements were taken. Leakage discharge was quantified

volumetrically by collecting effluent in a graduated cylinder over a fixed time interval, while the corresponding upstream pressure was read from the calibrated gauge. The procedure was repeated across all pressure increments and for all test media and orifice sizes.

Pressure-Gauge Calibration

Prior to experimentation, the pressure gauge was calibrated against a GDS pressure/volume controller (soil mechanics laboratory). Known pressures in the range 10–130 kPa were applied, and paired readings (applied vs. gauge) were recorded. A calibration curve was constructed by plotting true applied pressure against the observed gauge reading (Figure 4) and used to verify gauge performance (and, if necessary, to adjust readings during data reduction).

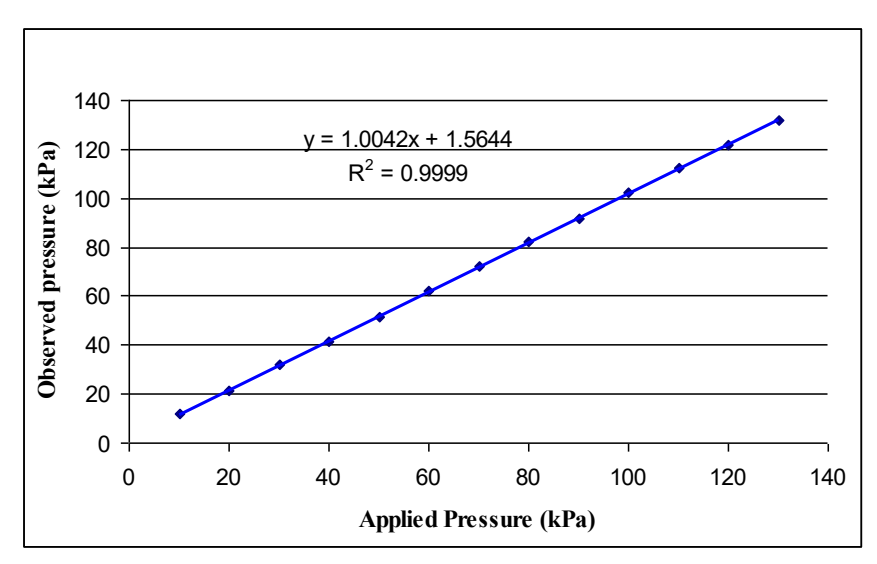


Figure 4 Pressure gauge calibration

4. Results and Discussion

4.1. Influence of the Surrounding Medium on Leakage

Four 12-mm steel pipe test sections, each containing a single circular orifice (diameters: 1, 3, 6, and 9 mm), were tested under three surrounding media: free discharge into air, submerged discharge into water, and discharge into saturated sand. For each configuration, paired measurements of upstream pressure head and leakage rate were acquired and plotted as leakage rate versus pressure head (Figures 5–8).

Across all orifice sizes, the presence of soil markedly attenuated leakage relative to free discharge. In several cases (notably for the 3, 6, and 9 mm orifices; Figures (6–8), the leakage rate into saturated sand was on the order of one-tenth of the corresponding value in air,

underscoring the strong influence of soil on outflow. This finding contrasts with the assertion by Walski and co-authors that the surrounding soil has negligible effect on leakage [1,20]. The reduction observed here is consistent with the additional hydraulic resistance and backpressure imposed by pore-scale flow through a granular matrix, as well as potential partial occlusion at the orifice—soil interface.

By comparison, submerged discharge into water produced leakage rates that were generally similar to those measured for free discharge, particularly for the 3, 6, and 9 mm orifices (Figures 6–8). Within the tested range, submergence did not induce a substantial deviation from the free-jet behavior, suggesting that the imposed internal pressure head dominated over any modest changes associated with the external hydrostatic environment. The 1 mm orifice (Figure 5) follows the same qualitative trend, though small departures can be expected at very low heads due to greater sensitivity to viscous effects and minor entrapped air.

Collectively, these results indicate that surrounding soil can substantially suppress leakage magnitudes, whereas simple water submergence exerts comparatively minor influence under the present test conditions. These observations have practical implications for leakage modeling and management, particularly when extrapolating laboratory free-discharge data to buried pipeline conditions.

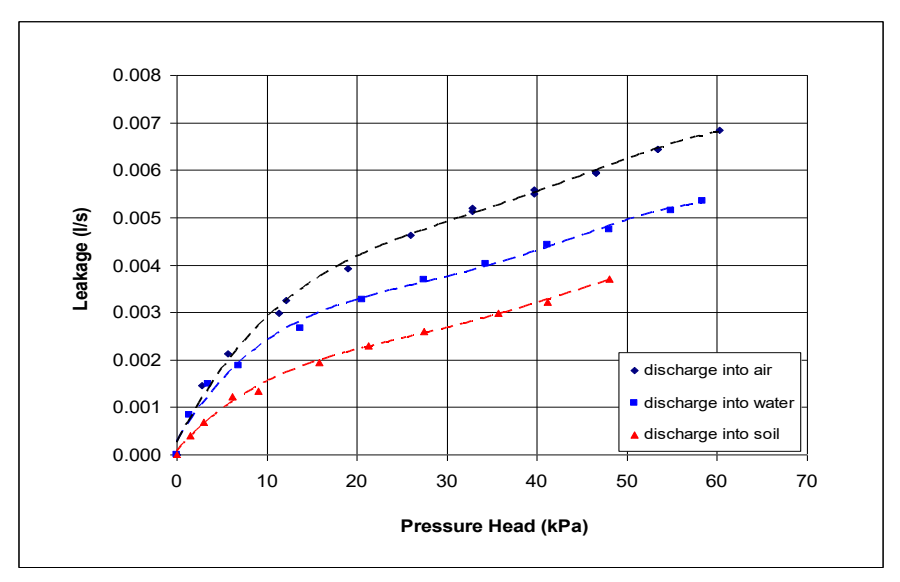


Figure 5. Leakage rate versus pressure head for the 1 mm orifice under different surrounding media (air, water, saturated sand).

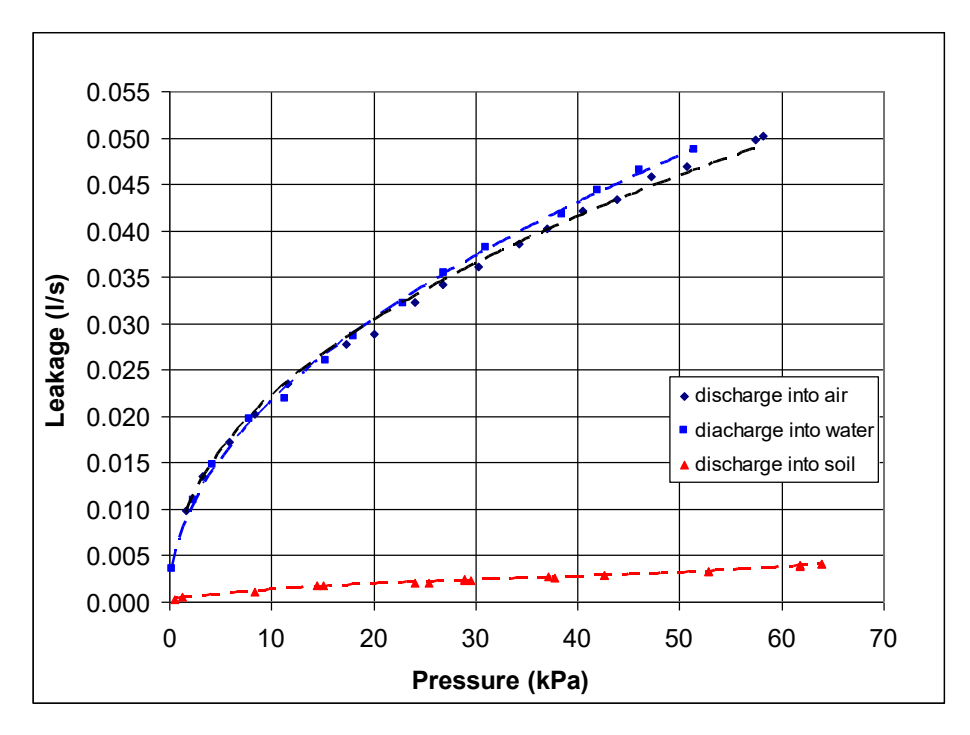


Figure 6. Leakage rate versus pressure head for the 3 mm orifice under different surrounding media.

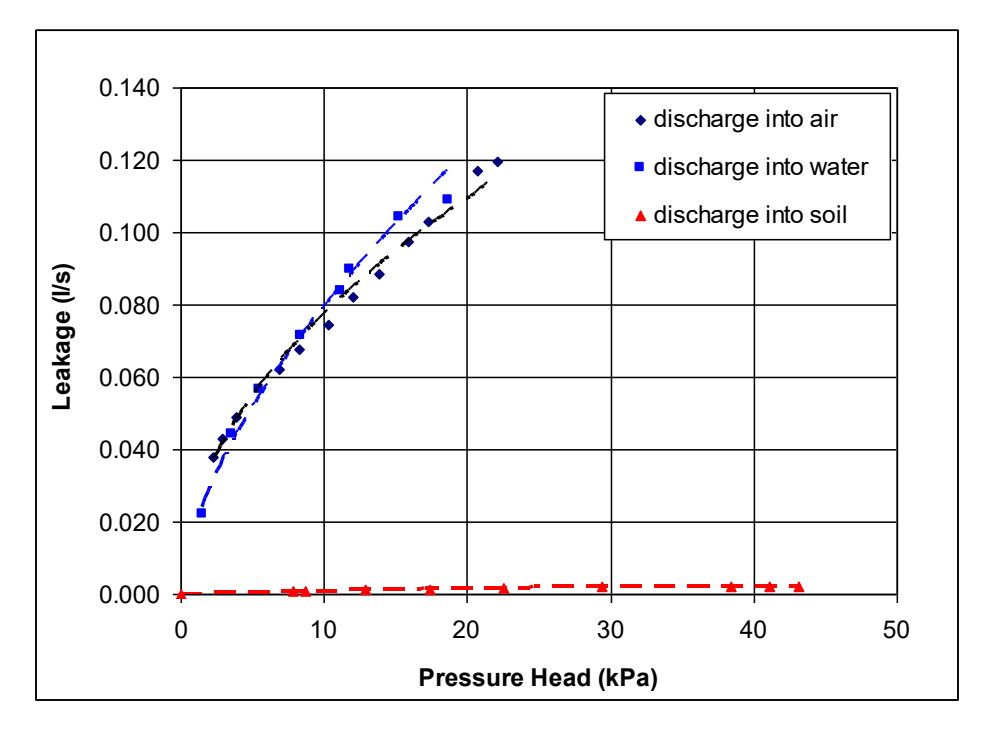


Figure 7. Leakage rate versus pressure head for the 6 mm orifice under different surrounding media.

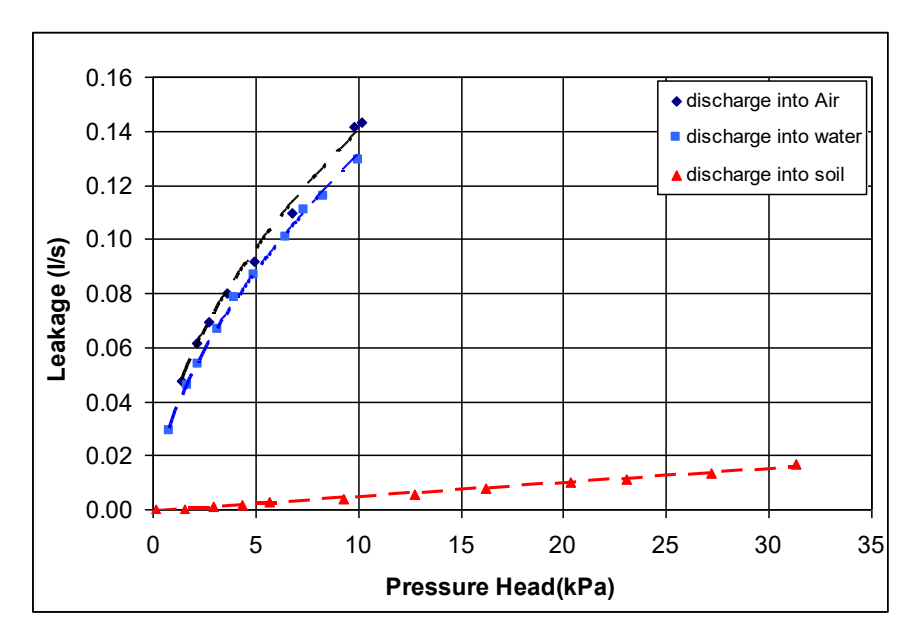


Figure 8. Leakage rate versus pressure head for the 9 mm open-ended pipe/orifice under different surrounding media.

4.2. Pressure-Leakage Relationship Across Surrounding Media

Because leakage depends on both pressure and boundary conditions, results were normalized to isolate the effect of pressure alone. A leakage factor, LF(p), was defined as the ratio of the leakage rate at pressure p to the leakage rate at 5 kPa for the same configuration:

$$LF(P) = \frac{Q(P)}{Q(5 \, kPa)} \tag{1}$$

With LF (5kPa) = 1. Figures 9–12 plot LF versus pressure head for each orifice and surrounding medium.

4.2.1. Air and water (free and submerged discharge)

For discharge into air, leakage scaled approximately with the square root of pressure, consistent with orifice-flow behavior $Q \propto \sqrt{\Delta P}$ (i.e., $LF \propto (\Delta P)^{0.5}$) An essentially identical 0.50-power trend was observed for submerged discharge into water (Figures 10–12), indicating that within the tested range the external hydrostatic environment did not materially alter the pressure dependence of the orifice outflow. Minor deviations at very low heads are expected for the smallest orifice (Figure 9) due to increased sensitivity to viscous effects and any residual air.

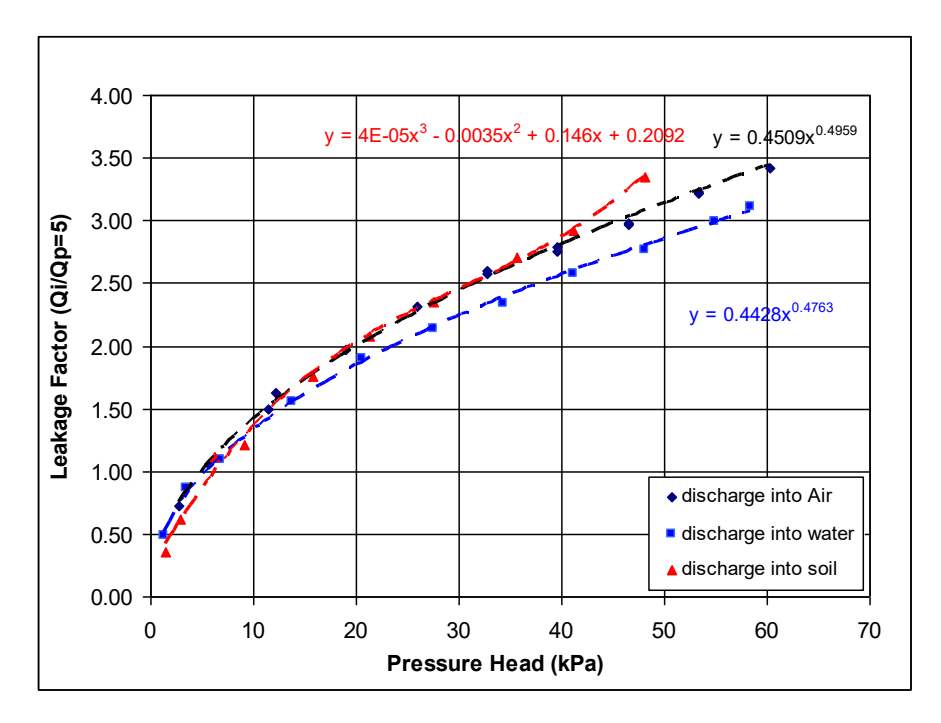


Figure 9. Pressure–leakage relationship for the 1 mm orifice under different surrounding media (air, water, saturated sand).

4.2.2. Saturated sand (buried/leaking condition)

In saturated sand, the pressure–leakage response differed markedly from free/submerged conditions. Over an initial range of pressures, leakage increased approximately linearly with pressure (i.e., LF \propto Δp). Beyond a threshold, however, further pressure increases produced disproportionate growth in leakage, signaling incipient soil instability. For the 3 mm orifice (Figure 10), this transition occurred at roughly 40 kPa. Such super-linear escalation is indicative of the onset of internal erosion processes (e.g., piping), where seepage forces exceed the buoyant weight and intergranular resistance of soil particles, or where a horizontal crack initiates and propagates upward until a continuous piping path forms [13].

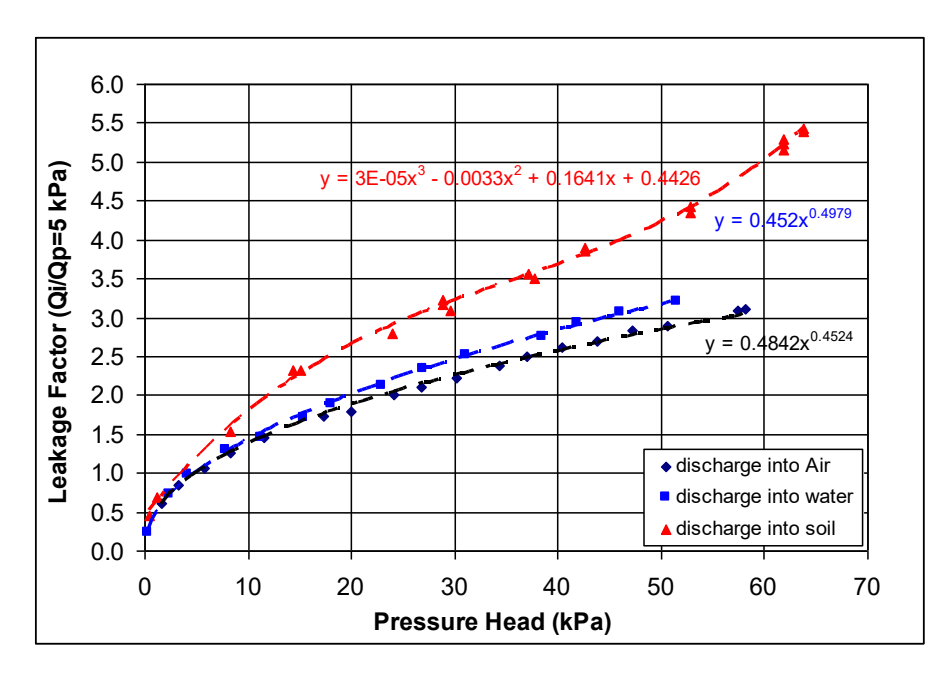


Figure 10. Pressure—leakage relationship for the 3 mm orifice under different surrounding media, highlighting super-linear growth above ~40 kPa in sand.

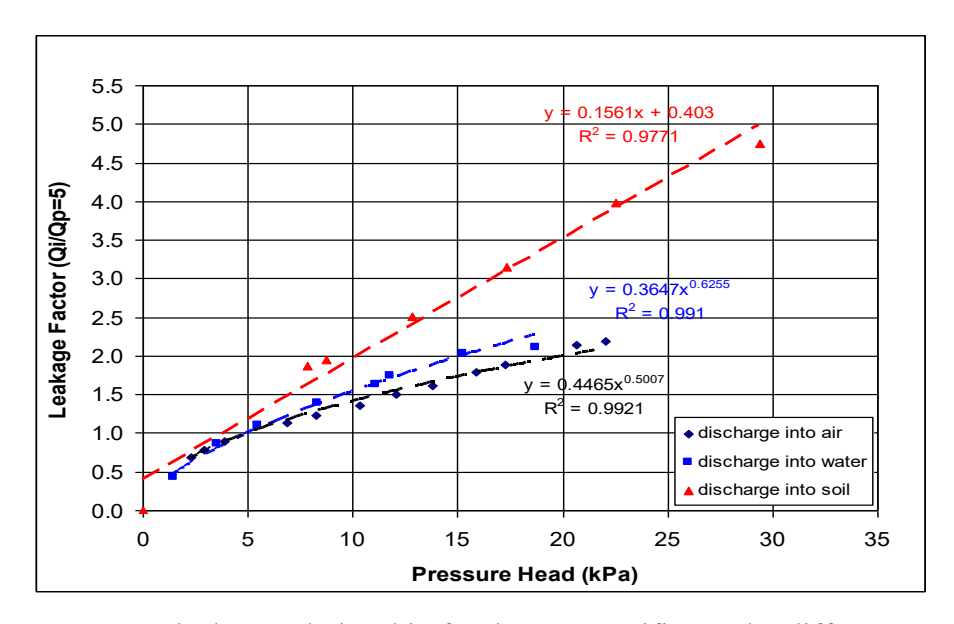


Figure 11. Pressure–leakage relationship for the 6 mm orifice under different surrounding media.

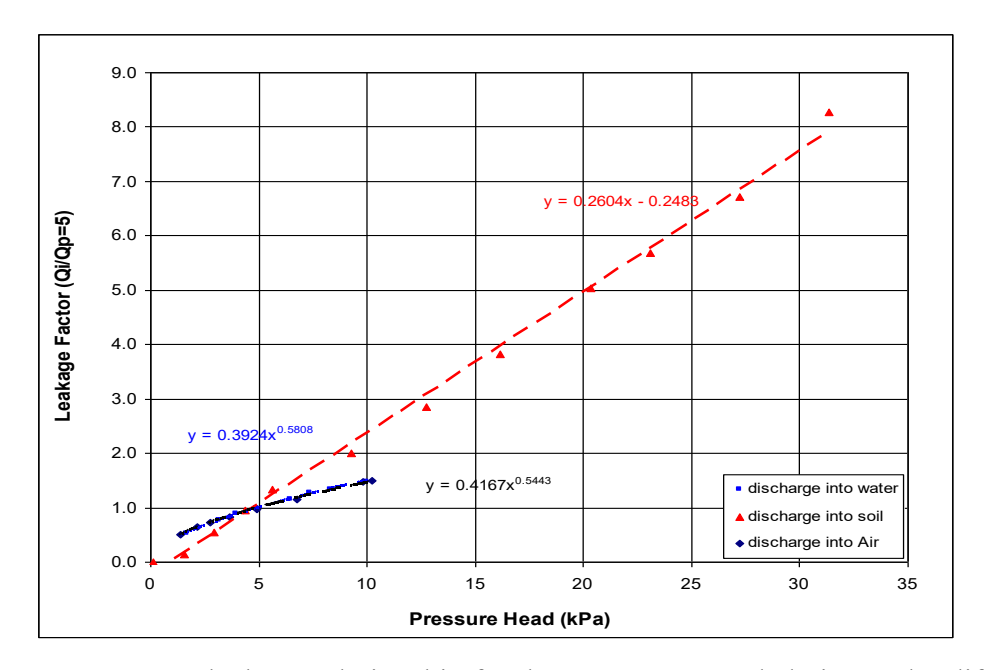


Figure 12. Pressure—leakage relationship for the 9 mm open-ended pipe under different surrounding media.

4.2.3. Piping onset and post-failure behavior (9 mm open-ended pipe)

Figure 13 documents piping for the 9 mm open-ended pipe discharging into saturated sand. Leakage initially increased linearly with pressure until around 32 kPa, at which point continuous "boiling" was observed: measured pressure fell rapidly while leakage rose sharply, stabilizing near 7 kPa with a peak leakage exceeding 0.14 L/s. A simple force-equilibrium estimate suggested a piping threshold near 12 kPa, but failure initiated at a substantially higher pressure. This discrepancy aligns with prior observations that piping initiation requires additional energy beyond that required to sustain piping, attributable to overcoming grain interlocking and fabric effects in the soil matrix [14].

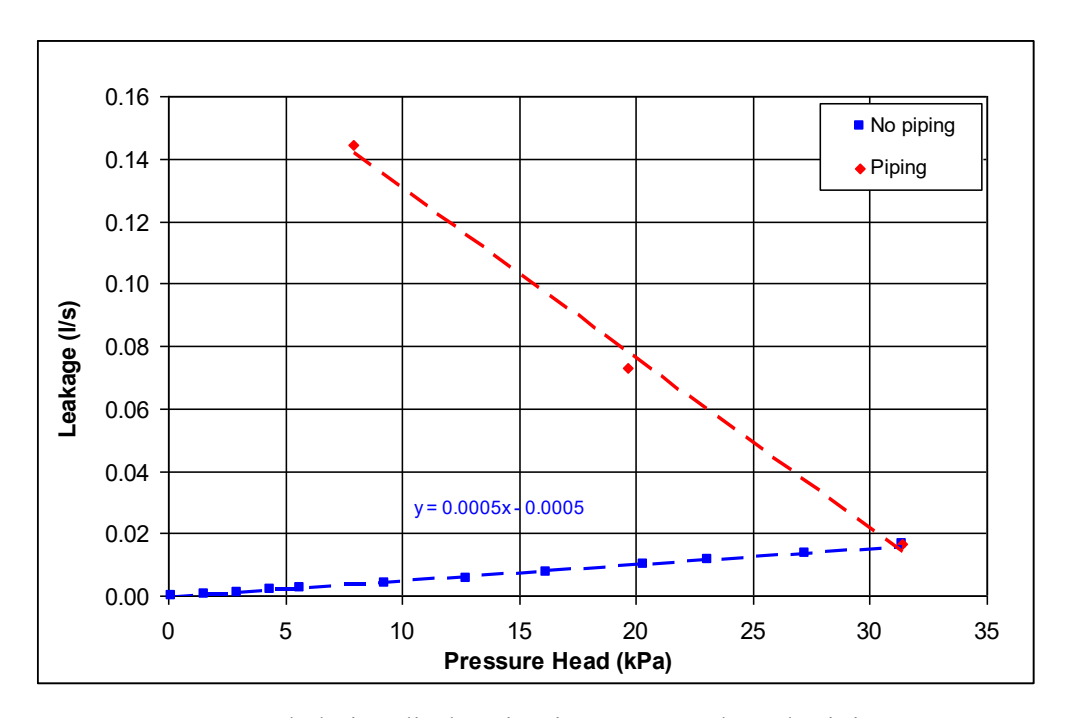


Figure 13. 9 mm open-ended pipe discharging into saturated sand: piping onset at ~32 kPa, followed by pressure collapse to ~7 kPa and leakage > 0.14 L/s

4.3 Coefficient of Discharge

The discharge coefficient, Cd was evaluated for orifices of 1, 3, and 6 mm diameter under three surrounding-media conditions: free discharge into air, submerged discharge into water, and discharge into saturated sand. For each test point,

$$C_d = \frac{Q}{A\sqrt{2gH}} \tag{2}$$

where Q is the measured leakage rate, A is the orifice area, g is gravitational acceleration, and H is the corresponding upstream head (or its equivalent from pressure). Results are plotted as Cd versus pressure head in Figures 14–16.

4.3.1. Effect of surrounding medium

Across all orifice sizes, Cd decreased sharply when discharge occurred into saturated sand compared with air or water. For the 3 mm orifice, for example, Cd dropped from approximately 0.65 under free discharge to about 0.045 in sand—an almost 93% reduction—corroborating the strong suppressive effect of the soil matrix on leakage. This reduction is plausibly attributable to (i) modification of the emerging jet by interaction with soil grains, which increases local head losses, and (ii) partial blockage at the orifice—soil interface that reduces the effective flow area.

In contrast, Cd for free and submerged discharge were nearly indistinguishable at moderate to high heads. For the 3 mm orifice (Figure 15), Cd ranged from approximately 0.65 to 0.67 for both conditions; for the 6 mm orifice (Figure 16), values were about 0.60–0.65. These observations are consistent with the classical behavior of drowned small sharp-edged orifices, for which Cd typically lies near 0.60–0.62 and is similar to free discharge under otherwise comparable conditions [11].

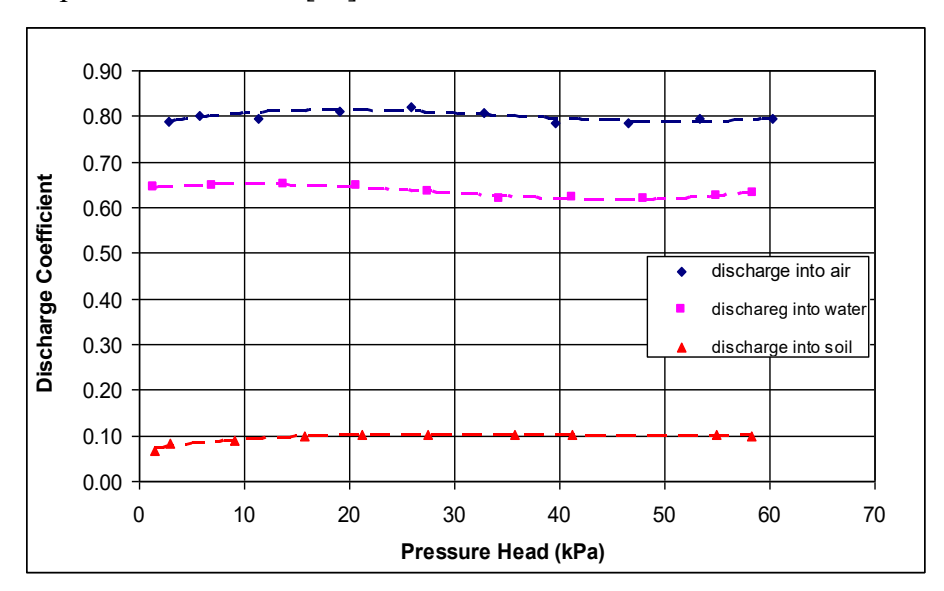


Figure 14. Discharge coefficient for the 1 mm orifice versus pressure head under air, water, and saturated-sand conditions.

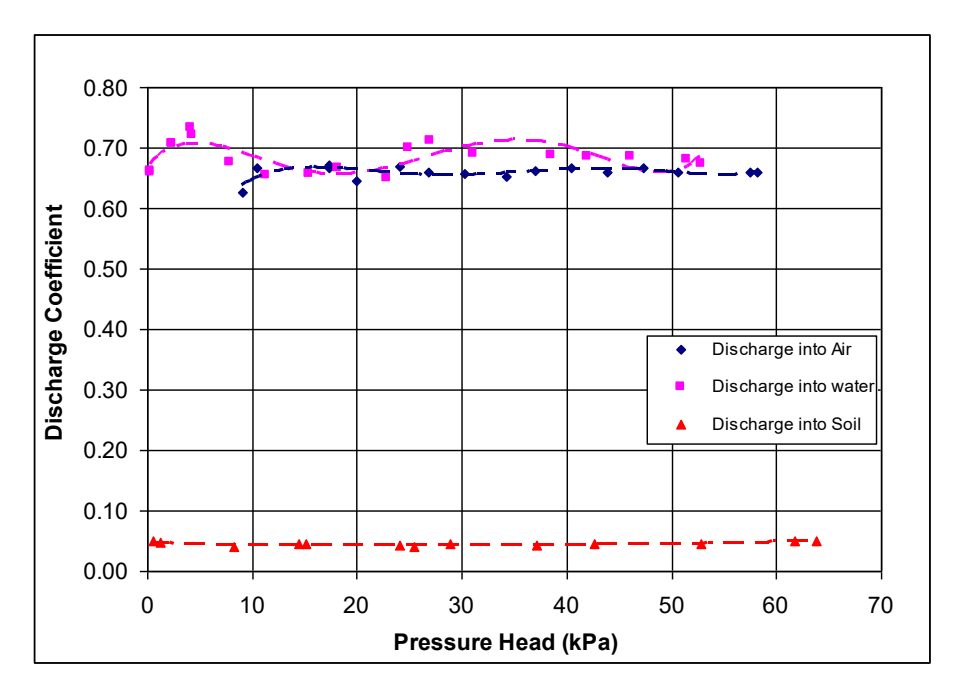


Figure 15. Discharge coefficient for the 3 mm orifice versus pressure head under air, water, and saturated-sand conditions.

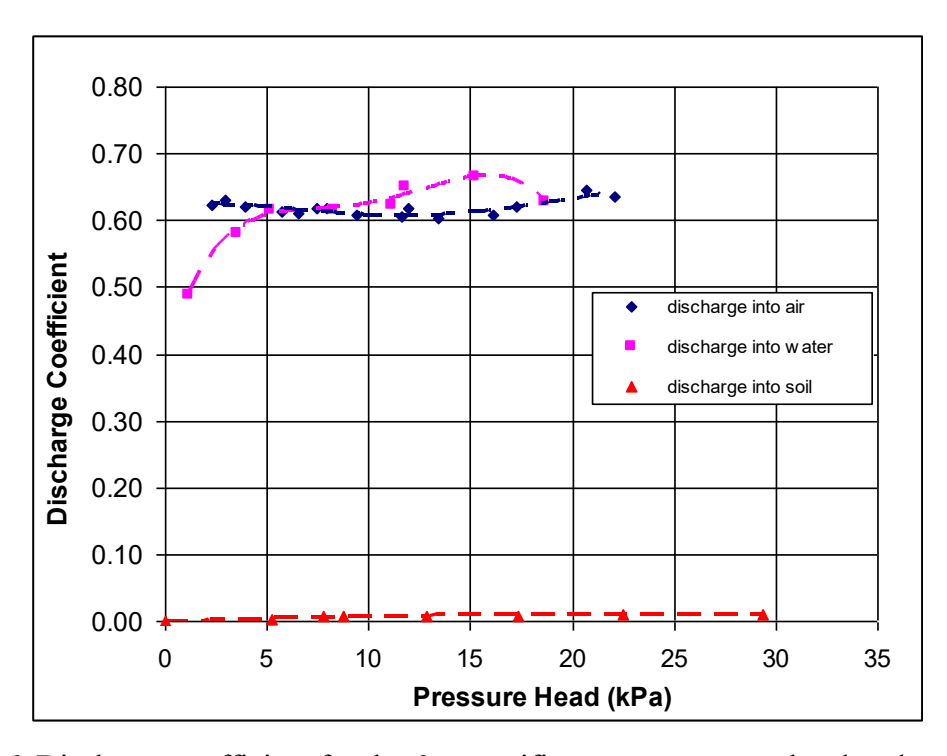


Figure 16. Discharge coefficient for the 6 mm orifice versus pressure head under air, water, and saturated-sand conditions.

4.3.2. Influence of diameter ratio

The impact of the geometric ratio β =do/Dp (orifice diameter/pipe diameter) was examined under free discharge into air (Figure 17). The internal pipe diameter used for this comparison was Dp = 9 mm, giving β =0.11,0.33, 0.66 for the 1-, 3-, and 6-mm orifices, respectively. The corresponding C_d values were approximately 0.79, 0.65, and 0.60, indicating a progressive decrease in C_d with increasing β . This trend suggests that as the opening occupies a larger fraction of the pipe wall, approach-flow nonuniformity and edge/geometry effects increasingly promote separation and energy dissipation at the orifice, thereby reducing the effective discharge efficiency.

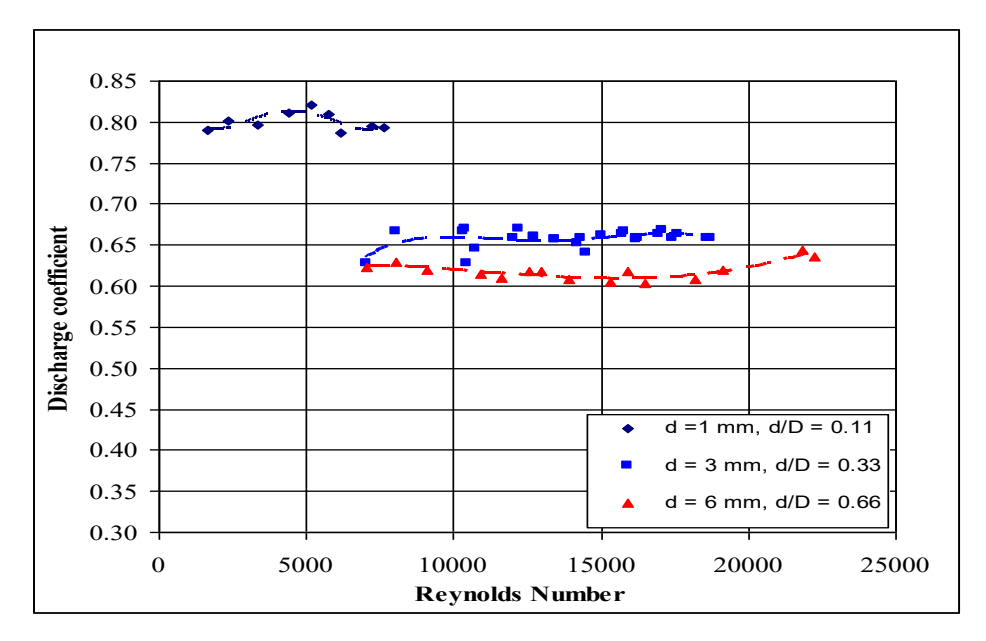


Figure 17. Discharge coefficient versus Reynolds number for different diameter ratios β under free discharge into air.

5- Conclusions

This study experimentally investigated the effects of surrounding media and orifice size on leakage behavior in pressurized pipes. The main conclusions are:

- 1. Leakage behavior depends strongly on the surrounding medium. While air and water discharges behave similarly, saturated sand significantly reduces leakage.
- 2. In soil, leakage increases linearly with pressure until a threshold, beyond which piping initiates, leading to uncontrolled leakage.
- 3. The discharge coefficient is drastically reduced in soil, with reductions exceeding 90% for larger orifices, indicating that soil particles reduce jet efficiency and effective orifice area.
- 4. Very small orifices (1 mm) showed minimal differences between media, as head loss was dominated by the orifice geometry.

These results underscore the importance of accounting for soil-pipe interactions and orifice size when interpreting leakage measurements and developing predictive models for buried water distribution systems.

References

[1] Walski, T., Chase, D., Savic, D., Grayman, W., Beckwith, S., & Koelle, E. (2004). Advanced Water Distribution Modeling and Management. Haestad Press.

- [2] May, J. (1994). "Pressure Dependent Leakage." *Proc. BICS Int. Conf. on Leakage Control.*
- [3] Lambert, A. O. (2001). "What do we know about pressure–leakage relationships in distribution systems?" *Proc. IWA Conf., Brno*.
- [4] Lambert, A. O., Fantozzi, M., & Shepherd, M. (2013). "Explaining, Assessing and Predicting Leakage; the 'N1' Concept." *Proc. IWA Water Loss Conference*.
- [5] Farley, M., & Trow, S. (2003). Losses in Water Distribution Networks: A Practitioner's Guide. IWA Publishing.
- [6] AWWA (2016). *M36: Water Audits and Loss Control Programs* (4th ed.). American Water Works Association.
- [7] Greyvenstein, B., & van Zyl, J. E. (2007). "An experimental investigation into the pressure–leakage relationship of some failed water pipes." *Journal of Water Supply:* Research & Technology—AQUA, 56(2), 117–124.
- [8] Cassa, A. M., & van Zyl, J. E. (2011). "Predicting the head–leakage slope for elastically deforming cracks in pipes." *Journal of Water Supply: Research & Technology—AQUA*, 60(1), 1–8.
- [9] van Zyl, J. E., & Clayton, C. R. I. (2007). "The effect of pressure on leakage in water distribution systems." *Water Management (ICE)*, 160(2), 109–114.
- [10] Rossman, L. A. (2000). *EPANET 2 Users Manual*. U.S. EPA (EPA/600/R-00/057).
- [11] Brater, E. F., King, H. W., Lindell, J. E., & Wei, C. Y. (1996). *Handbook of Hydraulics* (7th ed.). McGraw-Hill.
- [12] Idelchik, I. E. (2007). *Handbook of Hydraulic Resistance* (3rd ed.). Begell House.
- [13] Skempton, A. W., & Brogan, J. M. (1994). "Experiments on piping in sandy gravels." *Géotechnique*, 44(3), 449–460.
- [14] Niven, R., & Khalili, N. (1998). "Energy aspects of the initiation of piping." *Canadian Geotechnical Journal*, 35(5), 909–918.

Experimental Investigation of Leakage-Pressure Relationships in Water Distribution Systems: Effects of Surrounding Media and Orifice Size

- [15] Terzaghi, K., Peck, R. B., & Mesri, G. (1996). Soil Mechanics in Engineering Practice (3rd ed.). Wiley.
- [16] Kenney, T. C., & Lau, D. (1985). "Internal stability of granular filters." *Canadian Geotechnical Journal*, 22(2), 215–225.
- [17] Wan, C. F., & Fell, R. (2004). "Laboratory tests on piping of soils in embankment dams." *Journal of Geotechnical and Geoenvironmental Engineering (ASCE)*, 130(4), 373–380.
- [18] Colombo, A. F., Lee, P., & Karney, B. W. (2009). "A selective literature review of transient-based leak detection methods." *Journal of Hydro-environment Research*, 2(4), 212–227.
- [19] Thornton, J., Sturm, R., & Kunkel, G. (2008). Water Loss Control. McGraw-Hill/AWWA.
- [20] Walski, T., et al. (2006). "Leakage Modeling in Water Distribution Systems." *Journal AWWA*.

Citation: Majed O. Alsaydalani. (2025). Experimental Investigation of Leakage—Pressure Relationships in Water Distribution Systems: Effects of Surrounding Media and Orifice Size. International Journal of Civil Engineering and Technology (IJCIET), 16(5), 35-55.

Abstract Link: https://iaeme.com/Home/article_id/IJCIET_16_05_003

Article Link:

https://iaeme.com/MasterAdmin/Journal uploads/IJCIET/VOLUME 16 ISSUE 5/IJCIET 16 05 003.pdf

Copyright: © 2025 Authors. This is an open-access article distributed under the terms of the Creative Commons Attribution License, which permits unrestricted use, distribution, and reproduction in any medium, provided the original author and source are credited.

Creative Commons license: Creative Commons license: CC BY 4.0

⊠ editor@iaeme.com